# The use of scanning contactless conductivity detection for the characterisation of stationary phases in micro-fluidic chips

Zarah Walsh, <sup>a</sup> Mercedes Vazquez, <sup>ab</sup> Fernando Benito-Lopez, <sup>bc</sup> Brett Paull, <sup>ab</sup> Mirek Macka, <sup>a</sup> Frantisek Svec <sup>d</sup> and Dermot Diamond <sup>bc</sup>

- <sup>a</sup> Irish Separation Science Cluster, National Centre for Sensor Research, Dublin City University, Glasnevin, Dublin, 9, Ireland. E-mail: mercedes.vazquez@dcu.ie; Fax: +353 1 700 8021; Tel: +353 1 700 7602
- <sup>b</sup> Centre for Bioanalytical Sciences, National Centre for Sensor Research, Dublin City University, Glasnevin, Dublin, 9, Ireland
- <sup>c</sup> CLARITY: Centre for Sensor Web Technologies, National Centre for Sensor Research, Dublin City University, Glasnevin, Dublin, 9, Ireland
- <sup>d</sup> The Molecular Foundry, E.O. Lawrence Berkeley National Laboratory, Berkeley, CA, 94720, USA

#### Abstract

The use of scanning capacitively coupled contactless conductivity detection for the evaluation of the structural homogeneity and density of both packed and monolithic stationary phases in microfluidic chips is presented here for the first time.

#### Introduction

Since it was first described in the literature by Gillespie *et al.*,[1] a number of publications have reported the use of scanning capacitively coupled contactless conductivity detection (sC<sup>4</sup>D) as part of the characterisation procedure for both packed and monolithic stationary phases in capillary columns.[2–6] The advantage of this method is that it can easily detect small differences in the homogeneity of the stationary phase while being entirely non-destructive.[1] Despite the development and use of movable C<sup>4</sup>D on electrophoresis micro-fluidic chips reported by Wang *et al.* in 2003,[7] as yet there are no reports on the use of sC<sup>4</sup>D to characterise the homogeneity of packed and monolithic stationary phases within the channels of micro-fluidic chips.

Currently, methods for determining the quality of a stationary phase within a micro-fluidic chip are based on optical or scanning electron microscopy (SEM) or the application of the stationary phase for the separation of a test analyte. With the exception of confocal laser scanning

microscopy (CLSM), optical microscopy cannot visualise the interior structure of the stationary phase when it is not transparent. While CLSM can generate complete 3D images of stationary phase structures the technique is relatively laborious and expensive, and the stationary phase has to be stained with a fluorescent compound, [8] which is undesirable in many cases as this may affect the surface chemistry. For SEM, the channel must also be cut open for imaging, rendering it useless for further applications. Applying a stationary phase of unknown quality for the separation of potentially costly analytes is not an optimal solution either, although it is the best of the currently available options for determining the quality of the stationary phase while still being able to employ it for further use.

It is with this in mind that we propose the use of commercially available on-chip contactless conductivity detectors for the nondestructive characterisation and detection of micro-scale heterogeneities in packed and monolithic stationary phases. Two examples are presented: (1) Ni-Immobilised Metal Affinity Chromatography (IMAC) resins packed in poly(methyl methacrylate)/pressure-sensitive adhesive (PMMA/PSA) micro-fluidic chips; (2) poly(styrene-co-divinylbenzene) monoliths synthesised in situ in the channels of a cyclic olefin copolymer (COC) injection mouldedmicro-fluidic chip.

# 1. Particle packed stationary phases in PMMA/PSA microfluidic chips

Affinity columns for future application in the extraction and preconcentration of histidine-tagged proteins were prepared in PMMA/PSA chips by packing Ni(II)-IMAC resins in micro-fluidic channels. The resulting packed columns were then characterised by sC<sup>4</sup>D in order to assess the capabilities of this non-destructive, non-invasive technique for determining the packing density along the column.

The micro-fluidic device depicted in Fig. 1A (28 x 16 mm), containing three independent channels, was fabricated by laminating four layers of PMMA and PSA. The micro-fluidic channels, which contained an embedded weir for entrapment of beads with diameters  $\geq$ 50 mm, were fabricated in the different polymeric substrates by using a  $CO_2$  ablation laser (see Fig. S1 in the ESI). A thin (125 mm thick) PMMA substrate was used as the bottom layer of the chip, ensuring an optimal signal-to-noise ratio from the  $C^4D$ . [9] In order to locate the specific positions along the length of the column at which  $C^4D$  measurements would be taken, several marks 1 mm apart were made along the chip with the  $CO_2$  laser (Fig. 1A). The IMAC resin was

then packed in the micro-fluidic channels and filled with 20 mM sodium phosphate buffer (pH 7.5) for sC4D measurements in stop flow mode (ESI†).

A commercial TraceDec C<sup>4</sup>D system (Innovative Sensor Technologies GmbH, Austria) coupled to copper sensing electrodes fabricated in-house was used for measurements. The chip was placed on top of the substrate containing the copper electrodes and, by sliding the chip from mark 0 to 11, the packed columns were sequentially scanned along their whole length, from beginning to end (Fig. 1A). In order to continue scanning another channel, the chip was simply displaced accordingly to the left or right. The resulting sC4D profiles are shown in Fig. 1B. As can be seen, the dramatic increase in the C<sup>4</sup>D response observed in the region between 6 and 8 mm for column packed in channel 1 (C #1), and between 6 and 7 mm for column packed in channel 2 (C #2), allows a straightforward determination of the end of the packed columns. However, the increase in the C<sup>4</sup>D response for C #1 is more gradual (718 mV at 6 mm, 1370mV at 7mm and 1828 mV at 8mm) than the one observed for C #2 (from 878 mV at 6 mm to 1853 mV at 7 mm). This indicates that C #1 was not as densely packed in the last ca. 2 mm as the rest of the column. Microscope images (PARISS, Lightform Inc., NC, USA) taken from the region close to the end of C #1 actually show the presence of large voids in the packing, as well as some air bubbles (Fig. 1C). In comparison, no clear voids are observed in the microscope images taken from the more densely packed part of the columns (Fig. 1D). Furthermore, the relative standard deviation (RSD) of the collected data calculated for each column gives an indication of the homogeneity along the length.[4] This value can then be directly compared between different columns allowing the relative homogeneity between stationary phases to be determined. Thus, the RSD values were calculated for each column considering only the 7 points included in the first plateau of the C<sup>4</sup>D profile, i.e., up to 6 mm. Those values are 9.6% for C #1 and 20.4% for C #2, which reveals a higher homogeneity of packing for C #1. In comparison, a RSD of 5.2% was obtained for channel 3, in which no column was packed. The differences observed in the packing homogeneity from one column to another, as well as within the same column, could be explained by the broad size distribution of the beads used for packing, as seen in Fig. 1D. Although the resin manufacturers claimed that the average particle size was 90 mm, measurements carried out with the PARISS system in several samples revealed a larger variation in particle sizes, ranging from approx. 10 to 100 mm (see Fig. S2 in the ESI). In addition, higher C<sup>4</sup>D values are observed for the points localised outside the packed columns in channels 1 and 2 (second plateau of sC<sup>4</sup>D profile) compared to channel 3 (no packing). One of the possible causes for this is the increase in the conductivity of the buffer resulting from the leaching of nickel ions from the IMAC resins observed earlier.[10]

Finally, it should be noted that even though large voids and air bubbles can be clearly seen in the packed columns by optical microscopy, provided that the chip substrate is transparent, no quantitative information on the variation of the packing density is easily obtained by this technique as opposed to sC<sup>4</sup>D.

## 2. Monolithic stationary phases in COC micro-fluidic chips

Following the evaluation of particle-packed beds using the sC<sup>4</sup>D technique, monolithic stationary phases synthesised directly within the channels of the micro-fluidic chip were then examined. When synthesising monolithic stationary phases in situ in micro-fluidic chips, or indeed any mould, it is important to know that, batch to batch of pre-polymer solution, the resulting synthesised monoliths are homogeneous and reproducible.

Here we have used sC<sup>4</sup>D to show that four poly(styrene-co-divinylbenzene) [poly(S-co-DVB)] monoliths synthesised directly in the channel of COC micro-fluidic chips from different batches of pre-polymer solutions have a similar degree of homogeneity along the length of the channel. The micro-fluidic chips themselves were prepared in-house using a procedure described by Mair et al.[11] and the channels were pre-treated prior to the monolith synthesis using a method similar to that outlined by Chen et al. (ESI).[12] The poly(S-co-DVB) monoliths were synthesised in the channel by visible light initiated polymerisation using a 470 nm light emitting diode (LED) array as the initiating light source (ESI).[13]

Directly after polymerisation the monoliths were flushed with acetonitrile and dried under nitrogen flow as this accentuates the difference between filled and empty areas within the channel. Fig. 2A shows a comparison between a filled and empty channel to highlight the difference, and no voids are obvious along the length of any of the filled channels indicating that the polymerisation was successful. From the microscope images (Meiji Techno UK Ltd, Somerset,UK), each channel looks the same, which would suggest that they are of the same quality. The optical micrographs, however, cannot show what is inside the channel, only that the walls are coated. A ruler was used to mark 1 mm increments along the side of the micro-fluidic chip. The chips were then placed on a commercially available micro-fluidic C<sup>4</sup>D platform purchased from e-DAQ Pty Ltd. (New South Wales, Australia) and the profiles were taken in stop-flow mode by moving the chips at 1 mm intervals over the electrodes on the detection

platform, as shown in Fig. 2B. The clamp on the platform helps to keep the chip steady while taking the measurements to ensure the detection point is always on the channel. In all cases, the channels were filled with deionised water before scanning, as this was previously shown to be the optimal condition for scanning of the stationary phase.[1,2] Due to its low conductivity and constant composition, any changes in conductivity observed by the detector are most likely to result from changes in the homogeneity of the stationary phase.

The result of this measurement on four different filled micro-fluidic chips is shown in Fig. 2C. According to Connolly *et al.* a higher conductivity response corresponds to a larger fluid volume between the electrodes, which can be due to larger pore volumes or voids.[3] Lower conductivity, therefore, means that there is less electrolyte between the electrodes due to smaller pore volume, which in turn is associated with narrower average pore diameters and void-free fillings.

In the obtained scans there are no significant increases or decreases in the conductivity along the length of any of the four channels, therefore the channels are filled to a similar degree. Calculation of the RSD shows that the values for each of the four columns are 7.6% (Z2), 3.8% (Z3), 11.1% (Z4) and 8.9% (Z6). This suggests a reasonably good overall consistency of the columns generated by the in situ polymerisation procedure. To confirm the integrity of the monolith as indicated by the sC<sup>4</sup>D profiles, scanning electron micrographs of the monoliths in the channels were necessary. Knowing, however, that the monolith homogeneity does not differ between batches it was only necessary to sacrifice one chip from the four shown for SEM imaging. The sacrificial chip was scored across the channel using a box-cutter, immersed in liquid nitrogen and then broken along the score mark in order to examine the cross-section of the channel. The resulting micrograph of the poly(S-co-DVB) monolith in the channel is shown in Fig. 2D and E. These images show that the channel is entirely filled with monolithic stationary phase (Fig. 2D) and that the monolith is well adhered to the walls (Fig. 2E). It can be seen clearly that the quality of the stationary phases in the micrograph corresponds to the quality inferred by the low RSD values obtained by sC<sup>4</sup>D. While the bottom layer of the COC micro-fluidic chip is thicker than that of the PMMA/PSA chip, in which the IMAC resin is packed (500 mm compared to 125 mm), there is little impact on the sC<sup>4</sup>D measurement sensitivity. Variations in the conductivity along the channel in the region of 20–30 mV are easily picked up by the detector, as can be seen in Fig. 2C. Hauser and Kuban have previously studied the dependency of chip bottom layer thickness on the sensitivity of the detection and found that thickness up to approx. 700 mm allow for sensitive detection of analytes, therefore the increase in thickness to 500 mm is not a significant issue.[9]

#### **Conclusions**

Scanning C4D is an excellent method for assessing the homogeneity of stationary phases, either particle-packed or monolithic, in the channels of micro-fluidic chips. This method is simple, non-destructive and provides a continuum of information along the entire channel, as opposed to commonly used SEM imaging. Additionally, it has been shown to perform well on chips based on different materials and bottom layer thicknesses. Moreover, the method can be employed using in-house modified and/or fully commercial instrumentation, and has been cross-validated with conventional optical microscopy and SEM techniques. Based on the above, on-chip sC<sup>4</sup>D shows great promise for application in the quality control of mass-produced stationary phases within micro-fluidic chips.

## **Acknowledgements**

Authors would like to thank P. Clarke and R. Thompson for the fruitful discussions. Financial support from Science Foundation Ireland (Grants No. 08/SRC/B1412 and 07/CE/I1147), the Industrial Development Authority, Ireland (IDA project #116294), Irish Research Council for Science, Engineering, and Technology (Fellowship No. 2089), Marie Curie Excellence Grants and Funding (MEXT-CT-004-014361), and Bristol-Myers Squibb is gratefully acknowledged. F.S. and analytical work performed at the Molecular Foundry, Lawrence Berkeley National Laboratory, were supported by the Office of Science, Office of Basic Energy Sciences, US Department of Energy, under Contract No. DE-AC02-05CH11231.

#### **Notes and references**

- [1] E. Gillespie, M. Macka, D. Connolly and B. Paull, Analyst, 2006, 131, 886–888.
- [2] E. Gillespie, D. Connolly and B. Paull, Analyst, 2009, 134, 1314–1321.
- [3] D. Connolly, V. O'Shea, P. Clark, B. O'Connor and B. Paull, J. Sep.Sci., 2007, 30, 3060–3068.
- [4] D. Connolly, L. P. Barron, E. Gillespie and B. Paull, Chromatographia, 2009, 70, 915–920.
- [5] T.D.Mai, H. V. Pham and P. C. Hauser, Anal. Chim. Acta, 2009, 653, 228–233.
- [6] D. Connolly, P. Floris, P. N. Nesterenko and B. Paull, TrAC, Trends Anal. Chem., 2010, in press.

- [7] J. Wang, G. Chen and A. Muck, Anal. Chem., 2003, 75, 4475–4479.
- [8] I. Nischang, G. F. Chen and U. Tallarek, J. Chromatogr., A, 2006, 1109, 32–50.
- [9] P. Kuban and P. C. Hauser, Lab Chip, 2005, 5, 407–415.
- [10] S. Sharma and G. P. Agarwal, Sep. Sci. Technol., 2002, 37, 3491–3511.
- [11] D. A. Mair, M. Rolandi, M. Snauko, R. Noroski, F. Svec and J. M. J. Frechet, Anal. Chem., 2007, 79, 5097–5102.
- [12] G. F. Chen, F. Svec and D. R. Knapp, Lab Chip, 2008, 8, 1198–1204.
- [13] Z. Walsh, P. A. Levkin, V. Jain, B. Paull, F. Svec and M. Macka, J. Sep. Sci., 2010, 33, 61–66.

# **Figures**

# Figure 1

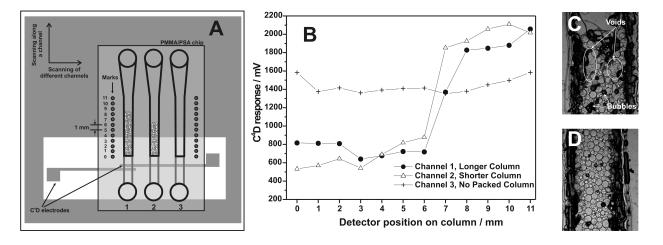


Figure 2

